Palestinian Medical and Pharmaceutical Journal

Bioavailability Enhancement of Abiraterone Acetate Through Quercetin-Loaded Nanoparticles

Suvarna Thorat[1],*, Meera Singh[2] & Manoj Tare[3]

Received: 12th Nov. 2024, Accepted: 17th Apr. 2025, Published: ××××, DOI: https://doi.org/10.xxxx

Accepted Manuscript, In press

Abstract: **Background:** Abiraterone acetate, a BCS Class IV biopharmaceutical drug with cytotoxic potential against cancer cells, faces limitations in its clinical use due to a short half-life and poor bioavailability. This work set out to employ nanoparticle technology to increase the bioavailability of abiraterone acetate by means of quercetin, a bioenhancer. Using the Eudragit RS-100 polymer and the emulsion solvent evaporation process, nanoparticles (NPs) were created, with a targeted particle size range of 236.8 to 389.22 nm.

Results: The produced nanoparticles demonstrated favourable *in vitro* characteristics, and the percentage of medicine discharged from all batches fell within acceptable thresholds. Notably, A549 cells exhibited a more positive response to a specific formulation (NP_2) with a higher bioenhancer loading. This unexpected finding suggested that the inclusion of abiraterone acetate into NPs contributed to maintaining the formulations' release profiles. This observation holds potential for reducing the dosage frequency of abiraterone acetate, thereby improving its clinical utility. **Conclusion:** In conclusion, the study indicates that the bioavailability of abiraterone acetate can be significantly improved through its encapsulation in nanoparticles, especially when combined with an herbal bioenhancer. The enhanced release profile observed, particularly in the case of NP_2, suggests a promising avenue for optimizing the proliferative effect of this anticancer medication.

Keywords: Abiraterone acetate, Eudragit RS-100, Quercetin, Nanoparticles.

Introduction

Throughout history, humans have extensively employed natural remedies. In the current era of nanomedicine, there is a growing trend in utilizing these natural products. Formulation scientists are increasingly drawn to phytochemicals, such as those found in the flavonolignan class, due to their numerous therapeutic benefits. However, the effective pharmacological application of these compounds faces several challenges, including inadequate absorption in the gastrointestinal tract, rapid degradation in bodily fluids, limited aqueous solubility, poor bioavailability, and challenges in intestinal permeability [1].

Numerous strategies are employed to enhance the absorption of medications in the intestines, encompassing bioavailability enhancers, prodrugs strategies and dosage forms such as liposomes and emulsions to improve permeability [2]. Co-administering active pharmaceutical ingredients (APIs) with natural compounds can enhance drug absorption and bioavailability. For example, piperine, a bioactive compound from black pepper, has been shown to enhance the bioavailability of curcumin by inhibiting glucuronidation in the liver and intestine [3]. Similarly, quercetin, a flavonoid, has been reported to improve the absorption of paclitaxel by modulating efflux transporters like P-glycoprotein [4]. These natural substances, termed "bioenhancers," hinder oxidative metabolism, efflux pumps, and the intestinal brush border membrane, thus increasing the bioavailability of co-administered medications [5].

There is a growing interest and medical need for non-pharmacological mechanisms include compounds like quercetin, piperine, zingiberin, genistein, cinnamon extract, glycyrrhizin, , ellagic acid, luteolin, and glycosides, niaziridin along with various other naturally occurring bio-enhancing agents [6,7]. Despite lacking pharmacological activity, they play a crucial role in minute quantities [8,9]. As a result, methods employing non-pharmacological bio-mechanisms to enhance the bioavailability of various medications are gaining attention [10].

Nano-bioenhancers, characterized by nanoparticles containing bioenhancers in the nanometer range, serve as drug delivery vehicles, inhibiting metabolic enzymes and facilitating permeability across gastrointestinal membranes. Various strategies aim to enhance medication bioavailability, ensuring consistent plasma concentrations and overcoming challenges associated with oral drug delivery, such as first-pass metabolism [11].

Abiraterone acetate is a prodrug that inhibits CYP17A1, reducing testosterone levels to treat castration-resistant prostate

1 Sinhagad College of Pharmacy, Vadgaon, Affiliated to Savitribai Phule Pune University, Pune, M.S., India.
* Corresponding author email: rani.suvarna29@gmail.com
2 E-mail: meerasingh2109@gmail.com
3 E-mail: manojstare75@gmail.com

cancer (CRPC). It is converted to its active form in the body, improving absorption and stability. Often used with prednisone to prevent adrenal insufficiency, abiraterone has shown significant clinical benefits in prolonging survival in metastatic CRPC. However, it may cause side effects like hypertension, liver toxicity, and cardiovascular issues, requiring careful monitoring. Research is also exploring its potential in other hormone-dependent cancers and combination therapies. [12].

This study develops a nanocarrier system for Abiraterone acetate using Eudragit RS-100 and quercetin (QUR) to improve its bioavailability. The QUR-loaded nanoparticles showed enhanced drug release, better absorption, and prolonged blood circulation, reducing dosage frequency and improving anticancer effects. [13].

Materials and Methods:

Materials

This study used Abiraterone acetate (CAS: 154229-19-3) for prostate cancer treatment, Quercetin (CAS: 117-39-5) as a bioenhancer, and solvents dichloromethane (CAS: 75-09-2) and acetone (CAS: 67-64-1) for nanoparticle preparation. Polyvinyl alcohol (PVA, CAS: 9002-89-5) served as a stabilizer, while Eudragit RS-100 (CAS: 24937-78-8) was used for controlled drug release all were purchased from LobaChemi, Mumbai.

Instrument used

Instruments used in the study included a melting point apparatus (to determine the melting point of the compound), UV spectrophotometer (for quantitative analysis and absorbance measurements), scanning electron microscope (SEM) (to analyze surface morphology and particle size), differential scanning calorimetry (DSC) (to study thermal properties and stability), X-ray powder diffraction (XRPD) (to determine crystallinity and polymorphic forms), Fourier-transform infrared spectroscopy (FTIR) (for functional group identification and structural analysis), dynamic light scattering (DLS) (to measure particle size distribution and zeta potential), and high-performance liquid chromatography (HPLC) (for drug content analysis and pharmacokinetic studies). These instruments were employed for various characterization and analysis tasks, including drug content, morphology, stability, and pharmacokinetics.

Method

Preformulation study of Abiraterone Acetate

Identification of Abiraterone acetate by Melting point determination

The capillary tube containing the sample was inserted into a melting point apparatus. The heating rate was set to approximately 1-2°C per minute to ensure accurate measurement. The temperature at which the drug started to melt and fully melted was observed. The melting point was recorded as the temperature at which the drug completely transitioned from solid to liquid.

Saturation solubility determination

The saturation solubility of Abiraterone acetate was determined by adding an excess amount of the drug (e.g., 10 mg) to 10 mL of distilled water and stirring the mixture for 24 hours at room temperature to achieve saturation. Additionally, to evaluate the pH-dependent solubility, the drug's saturation solubility was also determined in buffers of varying pH (1.2, 4.5, 5.5, and 6.8), as these pH values are physiologically relevant and critical for dissolution studies. pH 5.5, in particular, was emphasized due to its importance in dissolution testing. After equilibration, the solution was filtered using a 0.45 µm membrane filter. The concentration of the drug in the saturated solution was determined by UV spectrophotometry at its maximum absorption wavelength [14]

Formulation of nanoparticles by Emulsion Solvent Evaporation Method using Quercetin

Quercetin (natural bioenhancer, 5 mg), Abiraterone acetate (API, 10 mg), Eudragit RS-100 (polymer, 20 mg), and other constituents were dissolved in a mixture of dichloromethane (DCM, 10 mL) and acetone (5 mL) under constant stirring at 300 rpm using a magnetic stirrer. The organic phase was stirred at room temperature until uniform dissolution was achieved [15,16]. In a separate step, an aqueous phase was prepared by dissolving polyvinyl alcohol (PVA, 1% w/v, 20 mL) in distilled water. This aqueous phase was added dropwise to the organic phase under continuous stirring to form an emulsion [17]. The organic phase and aqueous phase mixture was then sonicated using a probe sonicator for 6 minutes at an amplitude of 40% to reduce the droplet size and achieve nanosized emulsion. After sonication, the organic solvent was evaporated by continuous stirring at 300 rpm on a magnetic stirrer for 4-5 hours to remove the dichloromethane and acetone completely. The resulting emulsion was centrifuged at 10,000 rpm for 30 minutes to separate the nanoparticles from the remaining supernatant. The nanoparticle emulsion was then stored at 4°C for 48 hours to stabilize before undergoing lyophilization. The lyophilized nanoparticles were stored in a desiccator until further characterization [18,19]. The formulation parameters to be investigated during the development of the model drug nanoparticles (NP's) are outlined in Table 1.

Table (1): Formulation Composition of Quercetin-Loaded Nanoparticles (NPs).

Formulation Code	Drug (in mg)	Weight of Quercetin (in mg)	Amount of Polymer (Eudragit RS-100) (in mg)	Amount of Surfactant (PVA) (%w/w)
NP's_1	250	100	60	0.15
NP's_2		100	60	0.20
NP's_3		100	120	0.25
NP's_4		100	120	0.30

Characterization of Nanoparticles

Determination of particle size,

Symphatec employed the laser diffraction method to characterize both the Abiraterone Acetate macro solutions and the course Abiraterone Acetate powder. The determination of nanoparticle size values was conducted through the photon correlation spectroscopy method.

Polydispersity index (PDI) and Zeta potential values

To determine the PDI and zeta potential, dynamic light scattering (DLS) analysis was performed. Samples were diluted 1:100 with deionized water and analyzed at room temperature to measure both the size distribution (PDI) and the surface charge (zeta potential) of the nanoparticles. A sample volume of 1 mL was used for the analysis.

Drug content

Spectrophotometric analysis was utilized to quantify the API of the nanoparticles. A calibration curve was first constructed by preparing standard solutions of abiraterone acetate in the same phosphate buffer, measuring their absorbance, and plotting the concentration against absorbance values. To obtain a concentration of 1 g/ml, a beaker containing the 10 ml of phosphate buffer and 10 mg equivalent of abiraterone acetate nanoparticles sealed to prevent evaporation. After stirring the mixture with a magnetic stirrer for 30 min. 3 ml of solution was pipetted out. The absorbance of collected sample was measured using a UV- spectrophotometric method, and the concentration of drug was calculated.

Loading Efficiency

After introducing 10 ml of buffer and 10 mg of abiraterone acetate were added to the nanoparticle suspension. The solution was subjected to ultracentrifugation for 30 minutes (at 8,000 rpm) at 4°C using a cold ultracentrifuge to segregate the nanoparticles containing the drug. The UV-spectrophotometer was employed to quantify the free drug concentration, and the entrapment efficiency (%) was then calculated.

Surface morphology

The surface morphological characteristics of optimized nanoparticles were evaluated using SEM (Scanning Electron Microscope - Quanta 400F Field Emission). A metal stub was made and the samples were quickly attached to it using double-sided adhesive tape. Subsequently, samples underwent gold-palladium coating in a vacuum and were subjected to voltage ranging from 5 to 20 kV before being scanned and inspected through SEM.

Fourier transforms infrared spectroscopy

FTIR analysis was used to obtain an infrared spectrum of abiraterone acetate within isotropic excipient combination. The FTIR examination involved analyzing abiraterone acetate coarse powder, physical mixtures, and optimized nanoparticles to determine if there were any interactions between the drug and excipients. To eliminate residual moisture, the samples underwent vacuum drying. The absorbance of each sample was then scanned over the range of 2900- 500 cm^{-1} with a resolution of 4 cm^{-1}.

Differential scanning calorimetry

DSC measurements were conducted using the Shimadzu DSC-60, employing a heating rate of 20 °C per min within temperature range of 25 °C - 300 °C. Abiraterone acetate, physical combination powders, and optimized nanoparticles were each weighed at approximately 2 mg and placed in an aluminum pan, which was then crimped and sealed. DSC thermograms were recorded by a nitrogen flow rate of 100 mL per min, and calibration was performed using an indium thermometer. Each sample underwent three measurements, and the average values for the projected onset temperature and maximum peak temperature were recorded for each measurement.

***In vitro* drug release studies**

The In vitro release studies of abiraterone acetate from nanoparticles was estimated using Haemodialysis Bag dispersion method. The research on nanoparticles employed pH 5.5 phosphate buffer (P.B.) which was chosen to simulate the slightly acidic environment of the gastrointestinal tract, particularly the conditions in the stomach. For the nanoparticle study, 18 mg of the corresponding abiraterone acetate nanoparticles were mixed in 10 ml of pH 5.5 buffer, added to the haemodialysis bag, and positioned at the same ends. The 100-cc buffer mixture was stimulated at 100 rpm speed and maintained temperature at 32 ± 20oC within the lateral line cubicle along with the haemodialysis bag. Enclosure of the lateral queue booth was done to prevent any loss of the distribution standard. Equivalent volume of diffusion medium was replaced after drawing the diagram, either before or after the lateral line partition. Sampling was conducted for a duration of up to 24 hours, and the samples were analyzed using UV spectroscopy.

***In vivo* study**

Animal Experiments

The study's participants were male Wistar rats, with a weight range of 180–250 g. The animals were housed in the main animal facility of the university the night before the trial began, and they were allowed unfettered access to water while fasting.

***Ex vivo* Permeation and Confocal Imaging Studies**

Rats euthanized by cervical dislocation underwent the extraction of their small intestines. The procedure involved everting a tiny (8 x 10 cm) portion of the intestinal segment with a glass rod, filling it with the test drug solution (usually 1.0 ml), and then securing the ends with thread. A mixture of 2 mL of drug-loaded optimized nanoparticles (NP_2) and 20ml of Rhodamine B (0.05%) was agitated for 30 minutes to incorporate the dye into the nanoparticles. Due to Rhodamine B's photodegradation property, caution was exercised during sample preparation. Subsequently, 1 mL of the prepared sample was introduced into surgically removed rat intestinal sac and transferred into a phosphate buffer (pH 6.5) used as a diffusion medium. permeation study occurred in this cell for 6 hours, placed on the magnetic stirrer and the mixture was agitated at 300 rpm and maintain at 37 ± 0.5 °C. Various intervals were used to extract 1 mL of medium and introduce an equal volume of new phosphate buffer solution in order to maintain sink conditions. We used HPLC analysis to find just how much medicine was entering the intestinal sac. The intestinal sac was meticulously removed, cleaned, and microtomized after the permeation experiment ended. This was done to prepare the slides for confocal laser scanning microscopy imaging using Rhodamine B at 540 nm for excitation and 625 nm for emission.

***In vivo* Pharmacokinetic Studies**

Study Design and Blood-Sampling

To evaluate the pharmacokinetics of the drug during fasting, a single-dose, randomized strategy was implemented. Animals were orally administered with 10 mg of abiraterone acetate in the form of either drug-loaded optimized nanoparticles (NP_2) or a free drug suspension. Under light anesthesia in a CO2 chamber, blood samples collected at various time intermissions of 0.5, 1, 3, 6, 12, 16, 18, and 48 hours. After centrifuging of the samples for 15 minutes (at 10,000 rpm) to separate the plasma, a predetermined concentration of the internal standard was added. The drug was extracted from rat plasma (5ml) using a extraction method, where T-butyl methyl ether (20 ml) was added in a 1:4 ratio. After 5 minutes of vortexing to mix the samples thoroughly, they were centrifuged at 15,000 rpm for 30 minutes. A fresh Eppendorf tube was used to collect the organic portion of the

supernatant, which was subsequently evaporated. The internal standard substance and abiraterone acetate levels in rat plasma were determined by using HPLC by reconstituting the dried residue with the mobile phase and filtering the mixture through a membrane filter (0.22 µm).

Stability Studies

Stability assessments, specifically accelerated stability studies, were conducted on the drug-loaded nanoparticles, involving their preparation under diverse stability conditions. The nanoparticles were isolated and kept for three months under three different conditions: room temperature (30 ± 2°C), refrigeration (4 ± 2°C), and accelerated situations (40 ± 2°C and 75 ± 5% relative humidity). Observations were made on both drug content and the physical appearance during this period [20,21].

Result

Preformulation study of Abiraterone Acetate-

Identification of pure drug

Melting Point

The determined melting point of Abiraterone Acetate was 144˚C, falling within the literature-reported range of 144-145˚C. Consequently, it can be confirmed that the drug is of high purity.

Maximum Wavelength (λmax)

The abiraterone acetate solution was subjected to scanning within the 200-400 nm range in spectrum mode. An absorption peak of abiraterone acetate was observed at a wavelength of 255 nm as shown in figure 1. Calibration curve was plotted absorbance vs concentration as in figure 2, regression was found to be 0.99. The standard deviation (SD) was found to be 0.523 this lower SD values suggest more consistent and reliable measurements.

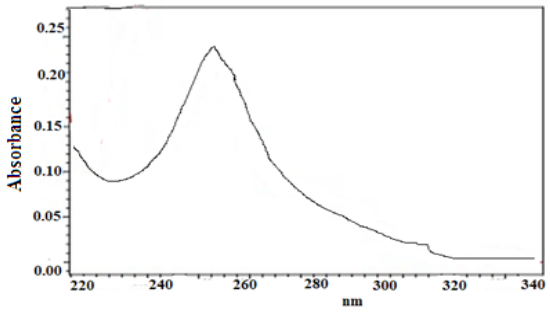

Figure (1): UV Spectra of Abiraterone Acetate (255 nm).

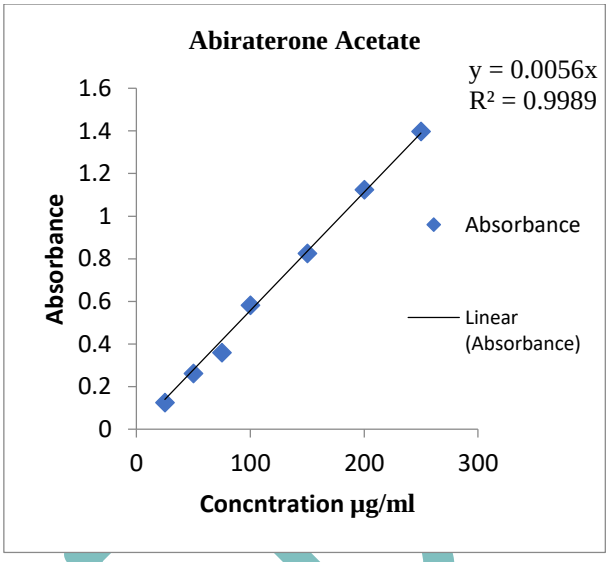

Figure (2): Calibration curve of Abiraterone acetate.

Saturation solubility study

The saturation solubility of abiraterone acetate was determined according to the method given by Higuchi and Conners in distilled water. The solubility of abiraterone acetate was 0.097 ± 0.032 mg/ml indicating the poor aqueous solubility of drug.

Characterization of Nanoparticles formulation

All the developed nanoparticles containing Abiraterone Acetate underwent characterization, including analysis of particle size, % of entrapment efficiency, zeta potential and SEM studies, as well as examination through FTIR, XRD, and DSC analyses.

Determination of drug content and Entrapment efficiency

Drug content and drug entrapment efficiency was calculated for all the formulation; data is summarised in Table 2. From the results NP's_2 showing highest loading efficiency hence selected as optimized formulation for further study.

Table (2): Drug content and drug entrapment efficiency of Abiraterone Acetate Nanoparticles.

Sr. No	Formulation	Drug Content (in %)	Loading Efficiency (in % w/v)
1	NP's_1	91.32 ± 0.766	94.76
2	NP's_2	89.33 ± 0.444	96.86
3	NP's_3	90.74 ± 0.045	95.75
4	NP's_4	92.54 ± 1.755	95.87

The loading efficiency ranged from 94.76 to 95.87, with the highest observed loading efficiency of 96.86 found in the NP's_2 group.

Particle size analysis

Visual inspection of various batches using binocular microscope, for particle size analysis in the prepared formulation batches shows i.e., 236.8 to 389.22 nm, Due to increase in polymer wall thickness, leads to formulation of larger size of nanoparticles. Among the formulations batch NP's_2 formulation showed ideal spherical nature with large surface area when compare to other batches.

Zeta sizer analysis for optimized batch (NP's_2) by using Zeta sizer (Malvern). The Z-average size of nanoparticles in the diluted sample with water was 236.8 nm, the Polydispersity

Index (PDI) value was 0.490, which was suitable for particle size estimation.

Zeta potential of Optimized Formulation NP's_2

The formed nanoparticles demonstrate electrostatic repulsion among them, and the presence of electric charge helps prevent particle aggregation. Zeta potential measurements were conducted under specified conditions, including a temperature of 24.9 °C, viscosity of 0.641 mPa.s, conductivity of 0.841 mS/cm, at a voltage of 3.3V, and an electrophoretic mobility of approximately -0.000094 cm2/Vs The zeta potential of -13.1 mV indicates low stability, as values below -20 mV suggest weak electrostatic repulsion, increasing the risk of aggregation. This suggests that while the nanoparticles are somewhat stable, further formulation adjustments may be needed to improve their stability

Morphological Studies by Scanning electron microscope

Results of surface morphology analysis showed that the NP's_2 was spherical in nature and that was induced by diffusion of solvents. Among all the batches of SEM analysis of NP's_2 batch was selected as the optimized formulation due to its ideal spherical nature of nanoparticles, as shown in figure 3.

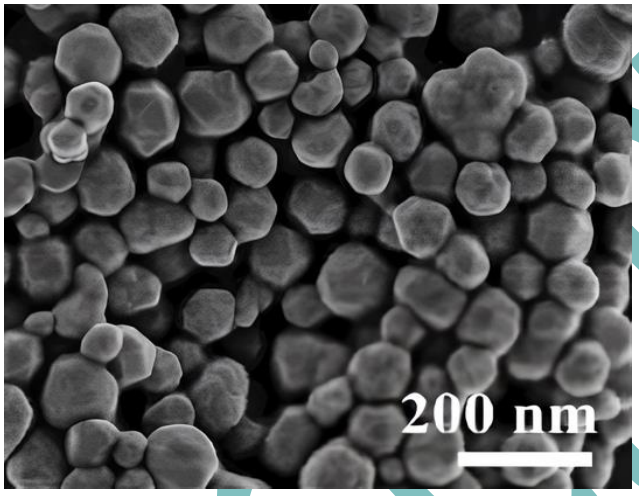

Figure (3): Results of SEM image of optimized formulation NP's_2

Analysis by Fourier Transform Infrared Spectroscopy

The infrared spectrum of the physical mixture was then compared with the spectrum obtained from the spectrophotometer. The scanning range was set from 400 to 4000 cm^{-1}, with a resolution of 4 cm^{-1}. Figure 4 shows the FTIR spectrum of Abiraterone acetate and FTIR spectra of quercetin.

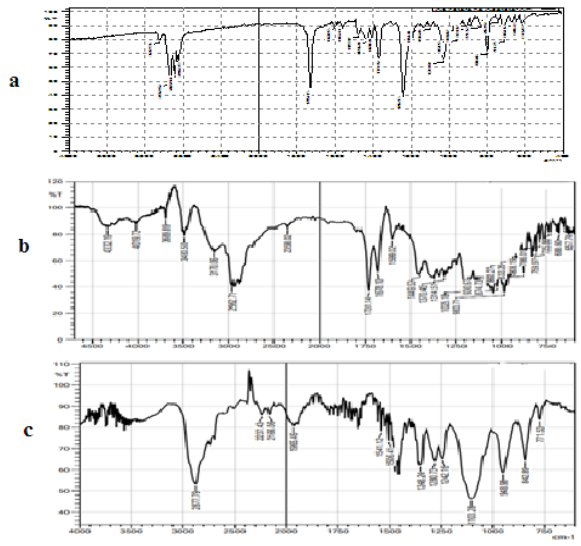

Figure (4): FTIR Spectra of a) Abiraterone Acetate (AB) b) Quercetin and c) Physical mixture of Drug and Quercetin.

The FTIR spectra shown in figure 5 of the physical mixture (c) show the retention of all major characteristic peaks of both Abiraterone Acetate (a) and Quercetin (b). There are no significant shifts, new peak formations, or disappearance of characteristic peaks, indicating **no chemical interaction** between the two components in the physical mixture. This suggests that the compounds are physically mixed without forming new chemical bonds

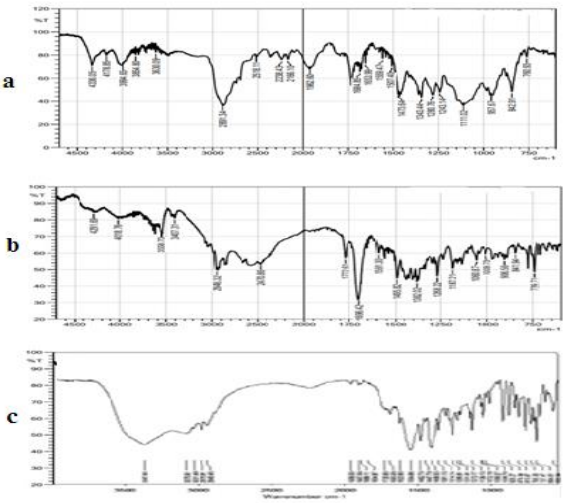

Figure (5): FTIR Spectra of a) Physical mixture Drug Eudragit RS-100 b) Drug, Quercetin and Eudragit RS-100 and c) Abiraterone acetate optimized nanoparticle formulation

FTIR Spectra of Physical Mixture of Abiraterone acetate and polymer

Upon analysing FT-IR spectra of polymers and its physical mixture with abiraterone acetate drug in figure it was determined that characteristic peaks corresponding to functional groups present in molecular structure of drug were not entirely within reference range. This observation confirms reactivity of the drug with polymer. This interaction further validates the choice of the polymer.

FTIR Spectra of Drug and polymer

No significant changes were observed in positions of characteristic absorption bands of different functional groups in drug. This observation strongly implies that drug maintains its characteristics without notable changes even in its physical mixture. The findings from FTIR spectra suggest an interaction between drug and polymer, revealing compatibility between drug and the polymers used.

Differential scanning calorimetry

DSC analysis of finalized NPs_2 formulation displayed an endothermic peak at 140°C, which closely aligns with the melting point of abiraterone acetate at 147°C, as illustrated in Figures 6(a) and 6(b). Despite a slight variance from the pure form, the thermogram indicates that there is no interaction between the abiraterone acetate and the polymer used. This observation aligns with findings from other studies by different authors, confirming the absence of interaction.

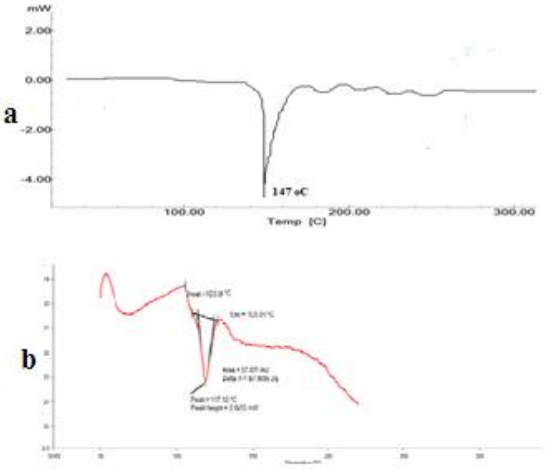

Figure (6): DSC thermogram of Abiraterone acetate drug and optimized formulation NP's_2

Table (4): Interpretation data.

Wavenumber (cm^{-1})	Interpretation
Spectrum a: Physical mixture of Drug and Eudragit RS-100	
~3300	O–H stretching (possibly from Eudragit and/or drug).
~2950–2850	C–H stretching (alkane groups in Eudragit and drug).
~1740	C=O stretching (ester group in Eudragit and drug).
~1600–1500	C=C stretching (aromatic ring in drug).
~1250–1000	C–O stretching (ester/ether groups).
Spectrum b: Drug, Quercetin, and Eudragit RS-100	
~3400	Broad O–H stretching (from Quercetin and Eudragit).
~2950–2850	C–H stretching (alkane groups in Eudragit and drug).
~1740	C=O stretching (ester group from Eudragit and drug).
~1650	C=O stretching (carbonyl in Quercetin).
~1600–1500	C=C stretching (aromatic ring in drug and Quercetin).
~1200–1000	C–O stretching (from ester/ether in Eudragit and Quercetin).
Spectrum c: Optimized nanoparticle formulation	
~3400	Retains broad O–H stretching (from Quercetin or Eudragit).
~2950–2850	Retains C–H stretching peaks (alkane groups in Eudragit).
~1740	Retains C=O stretching (from drug and Eudragit).
~1600–1500	Retains C=C stretching (from aromatic groups).
~1200–1000	Retains C–O stretching (from ester/ether groups).

In vitro release study

Percent drug release of drug and nanoparticles was summarised in to Table-5.

The data in Table 5 demonstrates that Abiraterone acetate nanoparticles (NP's) showed a significant increase in drug release compared to the free drug (API) over time, indicating enhanced release characteristics. Among the nanoparticles, NP's-2 exhibited the highest drug release, reaching 91.34% at 6 hours, suggesting improved solubility and sustained drug release compared to other formulations.

Table (5): In vitro drug release of Abiraterone Acetate drug and Abiraterone Acetate Nanoparticles.

Time in Hours	Drug API	NP's-1	NP's-2	NP's-3	NP's-4
0	0	0	0	0	0
1	12.95	34.38	50.58	37.53	45.34
2	15.84	45.54	62.53	46.54	53.32
3	19.33	52.43	72.43	54.32	59.34
4	23.54	57.34	84.45	59.34	65.38
5	25.47	60.34	88.53	64.23	71.48
6	27.49	62.54	91.34	70.31	79.58

Investigation of Ex vivo Permeation study and Confocal Microscopy Imaging studies

Ex vivo permeation assessments on rat intestine sections (duodenum and jejunum) revealed significantly higher drug permeation (3.75-fold increase; $p < 0.05$) with optimized NPs_2 of abiraterone acetate compared to pure drug suspension, indicating enhanced permeability via NPs. Confocal microscopy showed clear uptake of Rhodamine B-loaded NPs into the intestinal wall, with z-stacking indicating penetration depths up to 10 µm. NPs' nanometric size and intact appearance facilitated transcellular and paracellular transport, potentially enhancing systemic absorption of abiraterone acetate (figure 7).

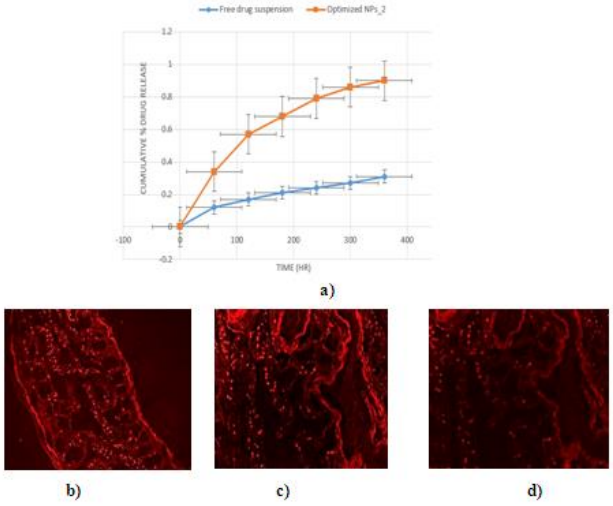

Figure (7): (a) Ex vivo permeation of Abiraterone Acetate from NPs_2 vs. suspension. (b) Confocal images of Rhodamine B-loaded NPs_2 uptake. (c, d) Z-stacking shows NPs_2 permeation up to 5 µm and 10 µm in intestinal tissue.

In vivo Pharmacokinetic Study

Figure 8 illustrates the pharmacokinetic profile of abiraterone acetate from drug suspension and optimized nanoparticles, showing significantly enhanced absorption characteristics ($p < 0.001$) with optimized NPs_2 compared to free drug suspension. Pharmacokinetic modelling favoured a one-compartment open model without absorption lag-time, supported by higher correlation coefficients, Akaike Information Criterion (AIC), and Schwarz Bayesian Criterion (SBC) values compared to a two-compartment model. Table 6 displays pharmacokinetic absorption parameters, revealing a remarkable 15.25-fold increase in Cmax and an 8.53-fold increase in AUC0–t with NPs_2 compared to free drug suspension. Additionally, optimized NPs_2 showed decreased T max, indicating faster drug absorption, and improved MRT and Ka, attributed to the lipid composition facilitating rapid absorption through gastrointestinal epithelial cells.

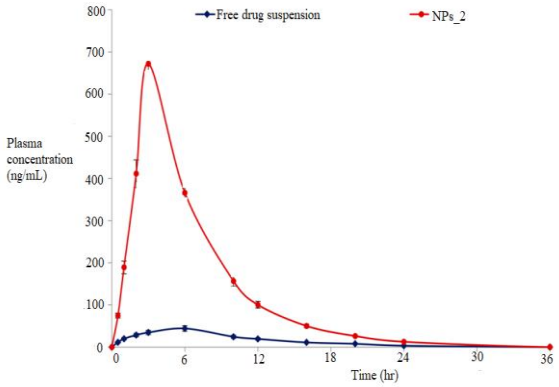

Figure (8): ADMET of Abiraterone acetate for both drug suspension and optimized nanoparticles

Table (6): Pharmacokinetic parameters of Abiraterone acetate drug and optimised nanoparticle in Wistar rats

Treatments type	Pharmacokinetic parameters					
	cmax (ng/ml)	AUC0-t (ng/mL/h)	Tmax (h)	Ke (h−1)	MRT (h)	T0.5 (h−1)
Abiraterone acetate drug	45.12 ± 7.47	501.67 ± 9.77	7.57 ± 0.35	4.35 ± 2.02	8.34 ± 0.88	5.83 ± 2.73
Optimized nanoparticles	773.13 ± 8.22	5258.99 ± 11.30	4.36 ± 0.76	3.72 ± 0.99	7.89 ± 2.12	4.92 ± 0.99

Stability Study

Stability study of abiraterone acetate optimized formulation was studied at various temperature conditions, as per ICH guidelines.

The stability study of the formulation over 90 days under room temperature (30±2°C), refrigeration (4±2°C), and accelerated conditions (40±2°C & 75±5% RH) showed clear and smooth appearance with minimal decline in drug content. The drug content reduced slightly from 90.93% to 90.22% at room temperature, 90.76% to 89.94% under refrigeration, and 90.56% to 89.97% under accelerated conditions. These results indicate good physical stability and minimal degradation, with refrigeration offering the best stability over three monthsThe stability studies revealed consistent drug content levels throughout the entire testing period, confirming the stability of the prepared groups. The standard deviation (SD) was found to be 0.898 this lower SD values suggest more consistent and reliable measurements.

Discussion

The preformulation study confirmed the purity of Abiraterone Acetate, as indicated by its melting point falling within the literature range. The UV spectra and calibration curve provided essential information for further analysis. The poor aqueous solubility of Abiraterone Acetate, as revealed by the saturation solubility study, highlights a major limitation in its bioavailability, necessitating the development of advanced formulation strategies. The stability studies consistently showed unchanged levels of drug content throughout the entire testing period, demonstrating the stability of the prepared formulations and ensuring their suitability for long-term use. NP's_2 exhibited the highest loading efficiency, suggest the formulation strategy involving specific excipients and processing conditions significantly enhanced the drug encapsulation, making it a promising candidate for improving therapeutic outcomes [22].

The range of particle sizes observed in the batches, particularly NP's_2, indicated successful nanoparticle formation which is crucial for ensuring uniform drug delivery and optimal bioavailability. Larger particle sizes in some batches may be attributed to increased polymer wall thickness. The spherical nature of NP's_2, observed through SEM analysis, supports its selection as optimized formulation. FTIR spectra indicated compatibility between the drug and polymer, validating the choice of Eudragit RS-100. The lack of significant changes in characteristic absorption bands in the physical mixture suggested no major alterations in drug characteristics indicating that the formulation process did not degrade the drug or interfere with its therapeutic properties. The XRD results confirmed the crystalline nature of the finalized formulation (NP's_2) with a lower intensity diffraction pattern, supporting its successful formulation. The DSC thermogram exhibited the peak associated to the melting point of Abiraterone Acetate in both the drug and the optimized formulation (NP's_2), suggesting the preservation of drug characteristics. In vitro drug release studies showed sustained release from the nanoparticles, with NP's_2 showing the highest cumulative release over time, emphasizing its potential for controlled drug delivery [23].

The enhanced absorption of Abiraterone Acetate from NP's_2 can be attributed to several key mechanisms. Nanoparticles improve drug absorption by increasing the surface area available for dissolution, thereby enhancing solubility and dissolution rates. Additionally, the use of Eudragit RS-100 and PVA in the formulation facilitates mucoadhesion, prolonging the residence time of nanoparticles at the absorption site. The small particle size of NP's_2 enables efficient uptake by enterocytes through endocytosis, bypassing efflux transporters such as P-glycoprotein, which often limit the absorption of poorly soluble drugs. Furthermore, nanoparticles can disrupt the tight junctions between epithelial cells, enhancing paracellular transport. These combined mechanisms contribute to the observed increase in C_max, AUC0-t, and faster T_max, ultimately improving the bioavailability of Abiraterone Acetate

Ex vivo permeation investigations and confocal microscopy images indicated a notable enhancement in drug permeability through the intestinal wall for NP's_2 in comparison to free drug suspension. The pharmacokinetic profile illustrated a significant improvement in drug absorption from NP's_2, showcasing increased C_max, AUC0-t, and a quicker T_max, highlighting the improved bioavailability of Abiraterone Acetate. The stability assessment affirmed that the optimized nanoparticles-maintained stability throughout the testing period, verifying their suitability for prolonged storage and application [24, 25].

In conclusion, the comprehensive characterization and evaluation of Abiraterone Acetate-loaded nanoparticles, particularly NP's_2, showcased their potential as an effective and stable formulation for enhancing the bioavailability of this cytotoxic anticancer drug. The results collectively suggest that the proposed nanoparticle technology could address the challenges associated with the poor aqueous solubility of Abiraterone Acetate, leading to improved drug delivery and potential therapeutic efficacy.

Conclusion

There are difficulties with daily screening of bio-enhancers that must be resolved. Large-scale production and regulatory oversight are the biggest barrier. In the finding based on the conventional Indian medical system, they propose a novel idea. Drug costs, toxicity, and other side effects will be reduced as a result of changes in this perspective. When given alongside numerous medications and nutraceuticals, many natural components have a noticeable boosting influence on bioavailability. In order to improve Abiraterone acetate's in vivo pharmacokinetic properties and decrease dosage frequency when treating cancer, this study produced a nanocarrier system containing the drug and a bioenhancer. Abiraterone acetate-QUR-loaded NPs were created and characterised for this use. The acquired results show that the drug's inclusion into NPs helped to maintain the formulations' release profiles, which may further lower the dosage frequency of abiraterone acetate. When administered via the in vivo approach using abiraterone acetate QUR-loaded NPs, the medication was more quickly absorbed and remained in the bloodstream longer. In comparison to plain drug-loaded NPs, area under plasma drug AUC were improved. Finally, it can be said that the proliferative effect of the anticancer medication in NPs can be enhanced by the addition of a bioenhancer.

Acknowledgment

The authors wish to express their gratitude to Sinhgad College of Pharmacy, Pune for their kind support during in vivo study and all other lab studies.

Funding

This research did not receive any specific grant from funding agencies in the public, commercial, or not-for-profit sectors.

Conflict of Interest

The authors declare no conflicts of interest related to this study.

Open Access

References

1] Theodosiou E, Purchartová K, Stamatis H, Kolisis F, Křen V. Bioavailability of silymarin flavonolignans: drug formulations and biotransformation. Phytochemistry reviews. 2014 Mar;13:1-8.

2] Maurya R, Vikal A, Patel P, Narang RK, Kurmi BD. Enhancing Oral Drug Absorption: Overcoming Physiological and Pharmaceutical Barriers for Improved Bioavailability. AAPS PharmSciTech. 2024 Oct 1;25(7):228.

3] Shoba G, Joy D, Joseph T, Majeed M, Rajendran R, Srinivas PSSR. Influence of piperine on the pharmacokinetics of curcumin in animals and human volunteers. Planta Medica. 1998;64(04):353-6.

4] Zhang S, Yang X, Morris ME. Flavonoids are inhibitors of breast cancer resistance protein (ABCG2)-mediated transport. Mol Pharmacol. 2004;65(5):1208-16

5] British Pharmacopoeia. Great Britain: The department of Health, Social Services and Public Safety 2007.

6] Tatiraju DV., Bagade VB., Karambelkar PJ., Jadhav VM., Kadam V. Natural bioenhancers: An overview. Journal of Pharmacognosy and Phytochemistry. 2013; 2(3):55-60.

7] Shaikh J., Ankola DD., Beniwal V., Singh D., and Kumar MR. Nanoparticle encapsulation improves oral bioavailability of curcumin by at least 9-fold when compared to curcumin administered with piperine as absorption enhancer. European journal of pharmaceutical sciences. 2009; 37(3-4):223-30.

8] Sangwan PL., Koul JL., Koul S., Reddy MV., Thota N., Khan IA., Kumar A. Piperine analogs as potent Staphylococcus aureus NorA efflux pump inhibitors. Bioorganic & medicinal chemistry. 2008;16(22): 9847-57.

9] Rathee P., Kamboj A., Sidhu S. Optimization and development of Nisoldipine nano-bioenhancers by novel orthogonal array (L27 array). International journal of biological macromolecules. 2016; 86:556-61.

10] Maser C, editor. Social-environmental Sustainability Series. CRC Press, Taylor & Francis Group; 2009.

11] Rathi PB., Kale M., Jouyban A. Thermodynamic Modelling and Solubility Study of Satranidazole in Different Monosolvents at Different Temperatures. Journal of Chemical & Engineering Data. 2021; 66(10):3745-56.

12] Nepolean R., Narayanan N., Subramaniyan N., Venkateswaran K., and Vinoth J. Colon targeted methacrylic acid copolymeric

nanoparticles for improved oral bioavailability of nisoldipine. Int. J. Biol. Pharm. Res. 2012; 3:962-7.

13] Toma L, Deleanu M, Sanda GM, Barbălată T, Niculescu LŞ, Sima AV, Stancu CS. Bioactive Compounds Formulated in Phytosomes Administered as Complementary Therapy for Metabolic Disorders. International Journal of Molecular Sciences. 2024 Apr 9;25(8):4162.

14] Adlin Jino Nesalin J, Rakshitha S, Ganesh NS, Vineeth Chandy. Determination of naringenin saturation solubility in diverse dissolution medium using UV-visible spectrophotometric analysis. Int J Res Publ Rev. 2024;5(9):3405-10

15] Kuna AK., Seru Ganapaty and Gadela V Radha. Analytical Method Development and Validation for the Estimation of Abiraterone and its Impurity in Pharmaceutical Formulation by RP-HPLC. Der Pharmacia Lettre. 2018; 10 (9): 19-31.

16] C. Schwarz. Solid lipid nanoparticles (SLN) for controlled drug delivery II. Drug incorporation and physicochemical characterization. J. Microencapsul. 1999; 16: 205–213.

17] A.A. Barba, S. Bochicchio, A. Dalmoro, D. Caccavo, S. Cascone, G. Lamberti. Polymeric and lipid-based systems for controlled drug release. Nanomaterials for Drug Delivery and Therapy. 2019; 57: 267–304.

18] J.E. Kipp. The role of solid nanoparticle technology in the parenteral delivery of poorly water-soluble drugs. Int. J. Pharm. 2004; 284:109–122.

19] J.-Y. Choi, J. Yoo, H.-S. Kwak, B. Nam, J. Lee. Role of polymeric stabilizers for drug nanocrystal dispersions. Curr. Appl. Phys. 2005; 5: 472–474.

20] M.M. Fiume, B. Heldreth, W.F. Bergfeld, D.V. Belsito, R.A. Hill, C.D. Klaassen, D. Liebler. Safety assessment of decyl glucoside and other alkyl glucosides as used in cosmetics. Int. J. Toxicol. 2013; 32: 22S–48S.

21] Mane V, Killedar S, More H, Tare H. Preclinical study on camellia sinensis extract-loaded nanophytosomes for enhancement of memory-boosting activity: optimization by central composite design. Future Journal of Pharmaceutical Sciences. 2024 May 1;10(1):66.

22] Mane V, Killedar S, More H, Nadaf S, Salunkhe S, Tare H. Novel Phytosomal Formulation of Emblica officinalis Extracts with Its In vivo Nootropic Potential in Rats: Optimization and Development by Box-Behnken Design. Journal of Chemistry. 2024;2024(1):6644815.

23] Mane VB, Killedar SG, More HN, Tare HL, Evaluation of acute oral toxicity of the Emblica officinalis Phytosome Formulation in Wistar Rats. International Journal of Drug Delivery Technology. 2022;12(4):1566-1570.

24] Deore S, Tajane P, Bhosale A, Thube U, Wagh V, Wakale V, Tare H. 2-(3, 4-Dihydroxyphenyl)-5, 7-Dihydroxy-4H-Chromen-4-One Flavones Based Virtual Screening for Potential JAK Inhibitors in Inflammatory Disorders. International Research Journal of Multidisciplinary Scope (IRJMS), 2024; 5(1): 557-567.

25] Deore S, Kachave R, Gholap P, Mahajan K, Tare H. Computational Identification of Methionyl-tRNASynthetase Inhibitors for Brucella melitensis: A Hybrid of Ligand-based Classic 3-Point Pharmacophore Screening and Structure Cavity Guided Blind Docking Approach. International Journal of Pharmaceutical Quality Assurance. 2023;14(4):1151-7.